Supplementary Material

Design and Synthesis of Nickel-Chromium Alloy Catalyst for Hydrogen Generation from Hydrazine Monohydrate

Jing He, Yuping Qiu, Sihuan Qin and Ping Wang*

School of Materials Science and Engineering, South China University of Technology, Guangzhou 510641, P.R. China

*Corresponding author.

E-mails: mspwang@scut.edu.cn (P. Wang)

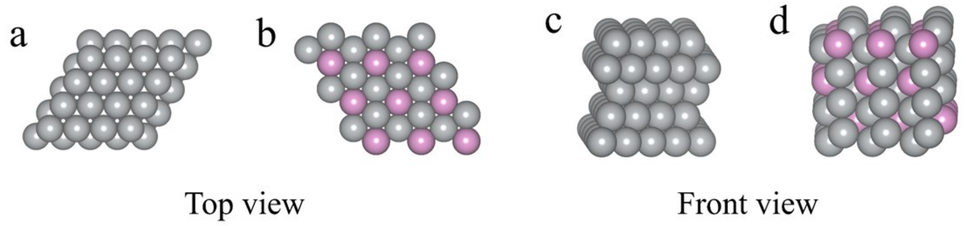

Figure S1. Top and front views of the modeled (a, c) Ni (111) and (b, d) Ni-Cr (111) surfaces. The gray and pink balls denote Ni and Cr atoms, respectively.

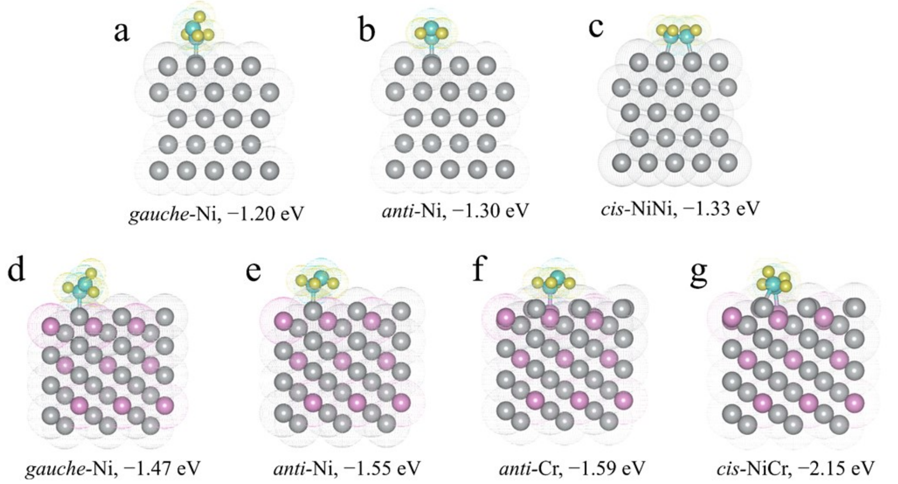

Figure S2. Computed adsorption conformations of N_2H_4 on (a-c) Ni (111) and (d-g) Ni_3Cr (111) surfaces and the corresponding adsorption energies.

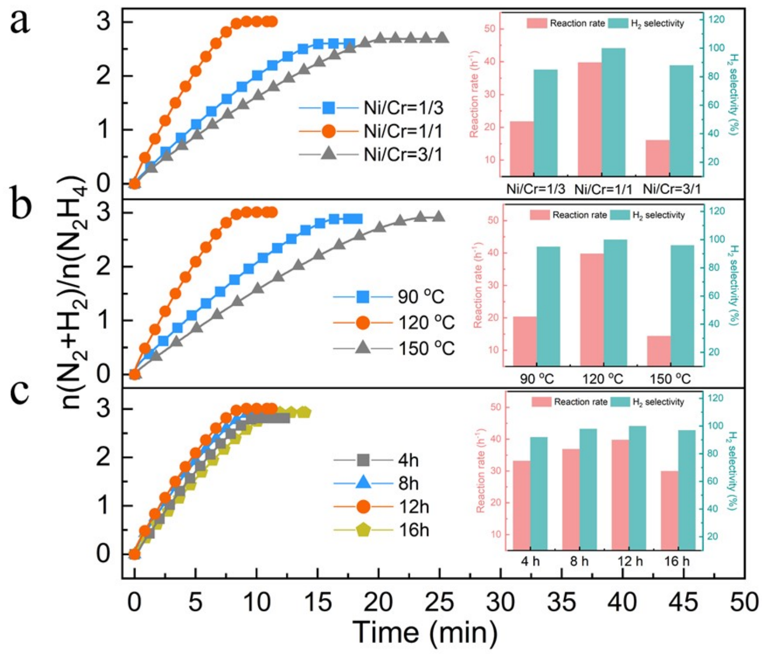

Figure S3. Effect of hydrothermal conditions on the catalytic properties of the samples for $N_2H_4 \cdot H_2O$ decomposition. (a) Ni/Cr feeding ratio; (b) reaction temperature; (c) reaction time. Insets show the reaction rate and H_2 selectivity of the samples prepared under different conditions.

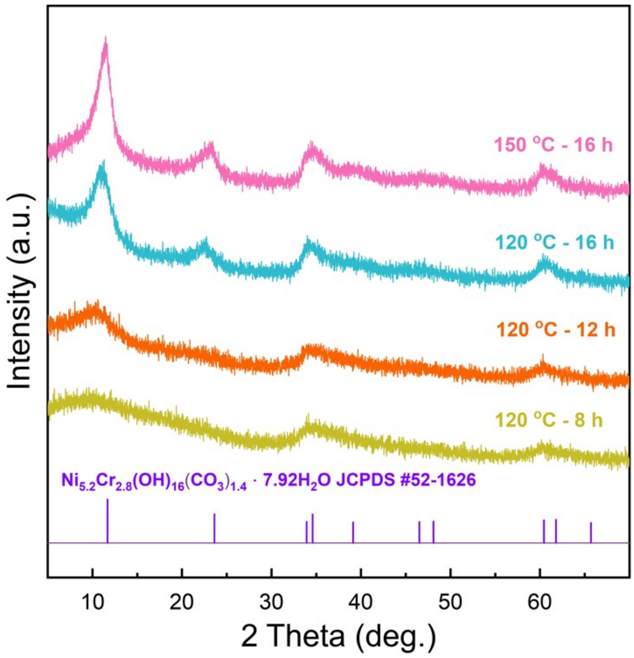

Figure S4. XRD patterns of the hydrothermal samples that were prepared under different conditions, with the Ni/Cr feeding ratio fixed at 1:1.

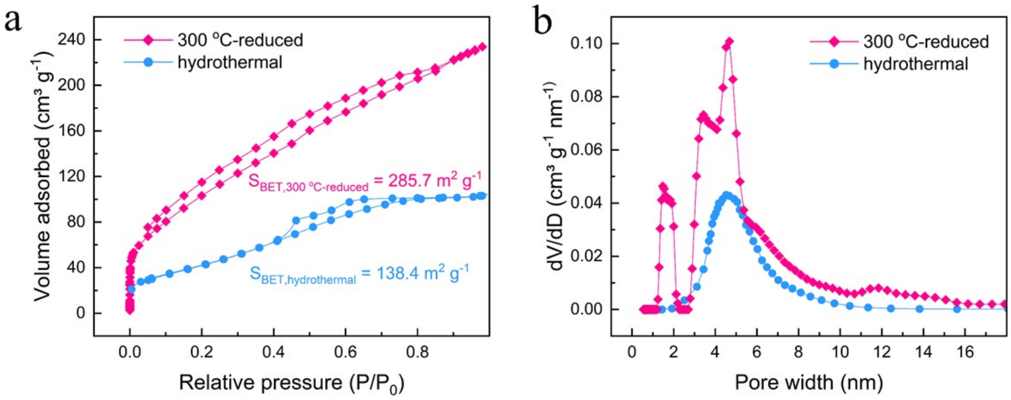

Figure S5. (a) N_2 adsorption-desorption isotherms and (b) the pore size distributions of the hydrothermal and 300 °C-reduced samples.

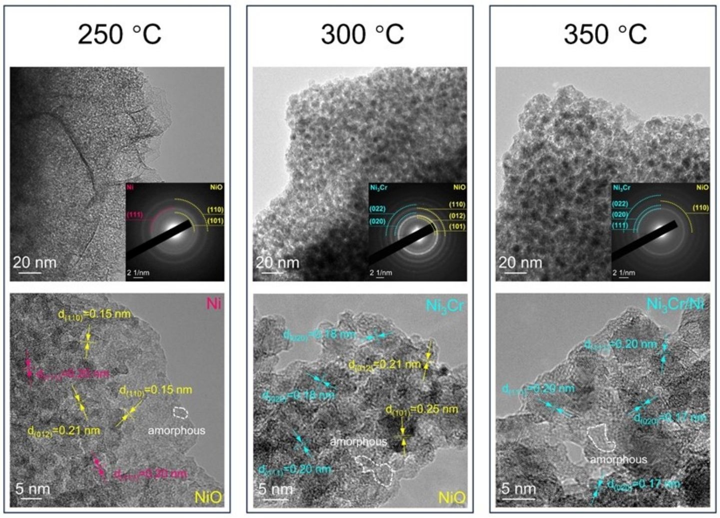

Figure S6. TEM and HRTEM images and SAED patterns (insets) of the reduced samples at different temperatures.

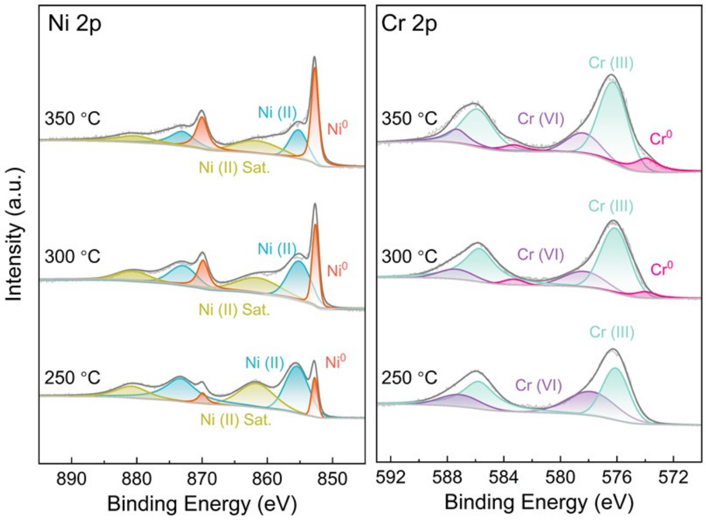

Figure S7. XPS results of the reduced samples at different temperatures in the Ni 2p and Cr 2p regions.

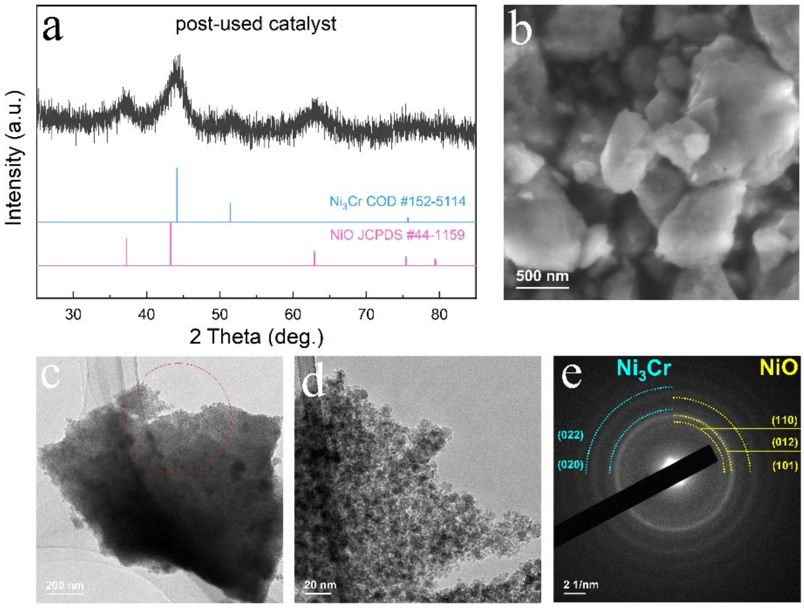

Figure S8. Morphology and phase structure characterization results of the post-used $Ni_3Cr/NiO-CrO_x$ catalyst: (a) XRD pattern; (b) SEM image; (c-d) TEM images; (e) SAED pattern.

Table S1. A comparison of the catalytic performance of non-precious metal catalysts for $N_2H_4\cdot H_2O$ decomposition. Activity attenuation after 10 cyclic usages; ^{a} 5 cyclic usages; ^{b} 3 cyclic usages.

Catalyst	Temperature (°C)	Reaction rate (h^{-1})	Selectivity (%)	Activity attenuation (%)	Reference
$Ni_{10}Mo$/Ni-Mo-O	50	54.5	97	<5	[1]
$Ni_4W/WO_2/NiWO_4$	50	33.0	99	<5	[2]
$Ni_{0.6}Fe_{0.4}Mo$	50	28.8	100	12^b	[3]
NiCo/NiO-CoO_x	25	5.49	99	30	[4]
NiFe/MgO	25	13.3	99	15^a	[5]
NiMoB-$La(OH)_3$	50	13.3	100	52	[6]
Ni-Al_2O_3-HT	50	2.0	93	40	[7]
2D NiFe/CeO_2	50	5.73	99	35	[8]
NiFe/$CeZrO_2$	50	24.7	100	48^a	[9]
Cu@Fe_5Ni_5	70	35.3	100	14^b	[10]
Ni_3Cr/NiO-CrO_x	50	39.8	100	<4	This work

References

1. Y. P. Qiu, G. X. Cao, H. Wen, Q. Shi, H. Dai, P. Wang, Int. J. Hydrogen Energy, 2019, **44**, 15110−15117.
2. Q. Shi, D. X. Zhang, H. Yin, Y. P. Qiu, L. L. Zhou, C. Chen, H. Wu, P. Wang, ACS Sustainable Chem. Eng., 2020, **8**, 5595−5603.
3. H. L. Wang, J. M. Yan, S. J. Li, X. W. Zhang, Q. Jiang, J. Mater. Chem. A, 2015, **3**, 121−124.
4. D. Wu, M. Wen, X. J. Lin, Q. Wu, C. Gu, H. Chen, J. Mater. Chem. A, 2016, **4**, 6595−6602.
5. W. Gao, C. Li, H. Chen, M. Wu, S. He, M. We, D. G. Evans, X. Duan, Green Chem., 2014, **16**, 1560−1568.
6. J. Zhang, Q. Kang, Z. Yang, H. Dai, D. Zhuang, P. Wang, J. Mater. Chem. A, 2013, **1**, 11623−11628.
7. L. He, Y. Huang, A. Wang, X. Chen, J. J. Delgado, T. Zhang, Angew. Chem. Int. Ed., 2012, **124**, 62950−6298.

8. D. Wu, M. Wen, G. Chen, Q. S. Wang, ACS Appl. Mater. Interfaces, 2017, **9**, 16103−16108.

9. H. Zou, Q. Yao, M. Huang, M. Zhu, F. Zhang, Z. H. Lu, Sustain. Energ. Fuels, 2019, **3**, 3071−3077.

10. J. Wang, Y. Li, Y. Zhang, Adv. Funct. Mater., 2014, **24**, 7073−7077.